TITLE: Evidence of early defects in Cajal–Retzius cell localization during brain development in a mouse model of dystroglycanopathy

AUTHORS: H. S. Booler, V. Pagalday-Vergara, J. L. Williams, M. Hopkinson, S. C. Brown

JOURNAL TITLE: NEUROPATHOLOGY AND APPLIED NEUROBIOLOGY

PUBLISHER: Wiley

PUBLICATION DATE: June 2017

DOI: 10.1111/nan.12376

Evidence of early defects in Cajal Retzius cell localisation during brain development in a mouse model of dystroglycanopathy

Booler H.S., Pagalday-Vergara V., Williams J.L., Hopkinson M. and Brown S.C.

Department of Comparative Biomedical Sciences,

Royal Veterinary College,

London NW1 0TU.

Author for correspondence

Email: scbrown@rvc.ac.uk.

Telephone: +44 20 74681212

Fax: +44 20 7468 5204

Running title: Early brain defects in the dystroglycanopathies

Number of words in the text: 4,173

Number of figures: 8

Abstract

AIMS: The secondary dystroglycanopathies represent a heterogeneous group of congenital muscular dystrophies characterised by the defective glycosylation of alpha dystroglycan. These disorders are associated with mutations in at least 17 genes, including Fukutin-related protein (*FKRP*). At the severe end of the clinical spectrum there is substantial brain involvement, and cobblestone lissencephaly is highly suggestive of these disorders. The precise pathogenesis of this phenotype has however, remained unclear with most attention focused on the disruption to the radial glial scaffold. Here we set out to investigate whether lesions are apparent prior to the differentiation of the radial glia.

METHODS: A detailed investigation of the structural brain defects from embryonic day 10.5 (E10.5) up until the time of birth (P0) was undertaken in the Fkrp deficient mice ($FKRP_{KD}$). Reelin, and downstream PI3K/Akt signalling pathways were analysed using Western blot.

RESULTS: We show that early basement membrane defects and neuroglial ectopia precede radial glial cell differentiation. Furthermore we identify mislocalisation of Cajal-Retzius cells which nonetheless is not associated with any apparent disruption to the reelin, and downstream PI3K/Akt signalling pathways.

CONCLUSIONS: These observations identify Cajal Retzius cell mislocalisation as an early event during the development of cortical defects thereby identifying an earlier onset and more complex pathogenesis than originally reported for the secondary dystroglycanopathies. Overall this study provides new insight into central nervous system involvement in this group of diseases.

Introduction

Type II lissencephaly (also referred to as cobblestone lissencephaly) is a type of neuronal migration disorder highly suggestive of a group of severe congenital muscular dystrophies, characterised by brain, eye and muscle defects. These disorders include Walker-Warburg syndrome (WWS) and Muscle-Eye-Brain (MEB) disease, both of which display a range of substantial structural brain abnormalities associated with defects in neuronal migration [1]. In addition to type II lissencephaly, WWS and MEB show cortical and cerebellar dysplasia, polymicrogyria and hydrocephalus, with evidence of dysmyelination on MRI [2, 3]. Many of these patients characteristically show a marked reduction in the glycosylation of alpha dystroglycan - an extracellular matrix receptor which is a key component of the dystrophin-associated glycoprotein complex [4]. These are now collectively referred to as secondary dystroglycanopathies since they carry mutations in genes involved in the processing of alpha dystroglycan rather than in the gene encoding for dystroglycan itself.

Alpha dystroglycan undergoes extensive O-mannosylation of its central mucin-rich domain, and it is these glycan chains that mediate binding to extracellular matrix proteins such as laminin [4], agrin [5-7], perlecan [8], and neurexin, effectively forming a link between the actin cytoskeleton and the extracellular matrix [9]. Altered binding to the extracellular matrix brought about by a reduction in the glycosylation of alpha dystroglycan is considered central to the disease process in the dystroglycanopathies and to date, mutations in 17 putative or determined glycosyltransferase genes have been associated with this group of diseases. These include *POMT1* [10], *POMT2* [11], *POMGNT1* [5], *LARGE* [12], *FKTN* [13], *FKRP* [14], *ISPD* [15, 16], *DPM1* [17], *DPM2* [18], *DPM3* [19], *POMK* [20], *GMPPB* [21], *B3GALNT2* [22], *GTDC2* [23], *TMEM5* [24], *B3GNT1* [25, 26] and *DOLK* [27, 28].

Fukutin-related protein (FKRP) is a putative glycosyltransferase, and mutations in *FKRP* produce a range of clinical phenotypes from WWS and MEB through to the late-onset limb girdle muscular dystrophy 2I (LGMD2I). In order to investigate the pathogenesis of the dystroglycanopathies further, we previously generated a mouse model of dystroglycanopathy which has a deficiency in fukutin-

related protein ($FKRP^{KD}$). This mouse recapitulates some of the features of MEB; displaying a profound reduction in the glycosylation of alpha dystroglycan at the pial basement membrane, associated with basement membrane defects and a neuronal migration disorder [29, 30]. In the dystroglycanopathies, this brain phenotype has been attributed to the inability of the radial glial end feet to maintain integrity of the pial basement membrane during the period of rapid cortical expansion; a process considered central to the neuronal migration defect in these disorders [31, 32].

However, there is now a substantial body of work which suggests that the meninges, traditionally seen as a protective layer covering the brain, play a key role in the production of basement membrane components, retinoic acid and chemotactic factors which are essential for normal corticogenesis [33-36]. Moreover, we have previously identified leptomeningeal disruption in newborn $FKRP^{KD}$ mice [37] potentially implicating the meninges in the pathogenesis of the brain defects associated with the dystroglycanopathies. In order to further investigate this we have now undertaken a detailed study of $FKRP^{KD}$ mice from E10.5 until P0. These investigations clearly show that basement membrane lesions and neuroglial heterotopia occur prior to radial glial disruption. There is a variation in the time of onset of these lesions, which could account for the range of severity observed at later stages, but lesions were identifiable in all embryos by E11.5. We further show that these defects occur around the time of Cajal-Retzius cell migration but are not associated with changes in the reelin and downstream PI3K/Akt signalling pathways.

Materials and methods

Animal models

All animal experiments were carried out under license from the Home Office (UK) in accordance with The Animals (Scientific Procedures) Act 1986 and were approved by the Royal Veterinary College ethics and welfare committee.

The FKRP-Neo^{Tyr307Asn} (FKRP^{KD}) has a neomycin selection cassette in intron 2 and a missense mutation in exon 3. The missense mutation (Tyr307Asn) has previously been shown to result in no discernable phenotype however, the presence of the neomycin selection cassette results in an 80% reduction in FKRP transcript levels [29]. This mouse was crossed with the GLAST^{cre}ERT2, to produce a mouse model with a knock down in FKRP with the potential to restore FKRP expression in response to tamoxifen administration.

Embryos

The morning of identification of the copulatory plug was taken to be E0.5. On the relevant day of gestation, the dam was euthanized by atlanto-occipital dislocation. The embryos were dissected out of the uterus, euthanized and fixed in ice cold Bouin's solution (Sigma), and transferred to 70% ethanol prior to processing. Prior to fixation, yolk sac or tail samples were collected and retained for genotyping.

Neonates

Mice were collected at P0 and killed by atlanto-occipital dislocation. The heads were removed and fixed in Bouin's solution (Sigma). The tails were collected for genotyping.

Histology

Following fixation, neonates and embryos were trimmed, processed and embedded in paraffin wax. Samples were serial sectioned at 5µm, with sections collected onto charged slides (Superfrost Plus, VWR, UK). Haematoxylin and eosin staining (H&E) was carried out using standard protocols.

Blinded semi-quantitative ranking of brain lesions was undertaken in embryos at each gestational time point, scoring lesion severity from zero (not present), through to 4 (marked).

Immunohistochemistry

Sections were deparaffinised and rehydrated. Primary antibodies used in the study were as follows: rabbit anti-brain lipid binding protein 1:300 (Millipore), mouse anti-reelin 1:1000 (clone G10, Abcam,

UK), rabbit anti-pan laminin 1:100 (Sigma, UK), anti-beta dystroglycan 1:150 (clone 43DAG1/8D5, Abcam, UK) and anti-alpha dystroglycan 1:300 (IIH6, Millipore, UK). Primary antibodies were diluted in phosphate buffered saline containing 0.05% tween 20 (Sigma) and incubated on sections for 1 hour at room temperature. Visualisation of the primary antibody was performed using the Envision system (DAKO). Sections were viewed using a DM4000B upright microscope (Leica, Germany) interfaced with Leica DC500 colour camera. Figures were compiled using Photoshop CS5 (Adobe, U.S.A.).

The number of Cajal-Retzius (CR) cells were counted in the rostral cortex, at the level of the corpus callosum. To ensure consistency, levels were matched using appropriate anatomical landmarks. The number of CR cells in the cortex were counted in each section. For each mouse, three serial reelin-stained sections (5µm apart) were counted and the mean number of CR cells per animal was calculated. Values were compared using a one way ANOVA with Dunnett's multiple comparisons.

Western blot

Whole brains were collected from E15.5 $FKRP^{KD}$ mice and lysed in (RIPA) buffer consisting of 50mM Tris-HCl pH 7.5, 1mM EDTA, 1% Triton X-100, 150mM NaCl, 1%SDS, plus a cocktail of protease inhibitors (cOmplete, ULTRA Mini EDTA free Roche) and phosphatase inhibitors (PhosStop, Roche). Protein concentration was measured using the BCA Protein Assay Kit (Thermo Scientific Pierce). Lysates were reduced and denatured and run on pre-cast polyacrylamide gels (Life Technologies), before transfer to PVDF membrane. Membranes were stained with antibodies to Akt (Cell Signalling, UK), PhosphoAkt (Cell Signalling, UK); Dab1 (Millipore, UK) and Lis1 (AbCam UK) and beta dystroglycan (Abcam, UK). Secondary horse radish peroxidase-conjugated goat anti-rabbit IgG and goat anti-mouse IgG antibodies (Jackson) were used to detect primary antibody binding, and staining was visualised with Pierce ECL western blotting substrate kit (Thermoscientific, UK). Membranes were imaged using the ChemiDoc MP system (BioRad, UK). Density analysis was carried out with Image Lab software (BioRad).

Genotyping

Genotype was confirmed by PCR. For FKRP^{KD} mice, primers were as follows FKRP forward - GTTGTGCTTAAACCACCTTC; FKRP neo forward - GGTGGGATTAGATAAATGCC; FKRP reverse - CTAGGAGGTTGAGGATGATGG.

Results

Defects in the basement membrane and disorganisation of neuronal precursors are present prior to rapid cortical expansion

Previous work in Pomgnt1$^{-/-}$, Pomt2$^{f/f;Emx1\text{-}Cre+}$ and Nestin cre-DG null embryos has suggested that the brain phenotype in the dystroglycanopathies is the result of a failure of radial glial cells to stabilise the basement membrane during a period of rapid cortical expansion [32, 38]. In order to further evaluate this we harvested brains from wild type and FKRP^{KD} embryos, at E10.5 and E11.5 (neuroepithelial stage), E12.5 (preplate stage) and E15.5 (middle of cortical expansion) to determine the point of onset of the neuropathologic phenotype.

Disruption to the preplate is identified in FKRP^{KD} mice early in brain development

A subtle brain phenotype, characterised by multifocal disorganisation of the pre-plate was identifiable in haematoxylin and eosin (H&E) sections in 60% of FKRP^{KD} embryos at E10.5 and 100% by E15.5. Figure 1 shows a semi-quantitative assessment of lesion severity from E10.5 to E15.5. Lesions were categorised as follows:- 0 = normal, 1 = focal defects in the pial basement membrane, with herniation of cells through the defects, 2 = multifocal defects in the PBM, herniation of cells through defects, 3 = moderate disorganisation of the developing cortex, limited or multifocal organisation of the cortical plate, 4 = significant disruption to the developing cortex, no differentiation of the areas of organisation, 5 = complete disorganisation of the developing cortex, no normal structures apparent.

These lesions most commonly occurred in the striatum of the lateral ganglionic eminence where at E10.5 in a proportion of embryos, irregularities at the interface between the LGE and mesenchyme

were observed (Figure 2). Immunolabelling of the IIH6 epitope of glycosylated alpha dystroglycan at E10.5 reveals there is strong, diffuse staining of the wild type neuroepithelium at this time point (Figure 2C). However, despite only a proportion of embryos exhibiting a morphologically obvious lesion at this time point, hypoglycosylation of alpha dystroglycan, demonstrated by an absence of IIH6 immunolabelling, was identified in all of the FKRP^{KD} embryos examined (Figure 2D). In addition, the neuroepithelial basement membrane, immunopositive for laminin, which was clearly identifiable in wild type embryos at E10.5, was not apparent in FKRP^{KD} embryos (Figure 2E,F).

By E11.5 multifocal disruptions of the neuroepithelium and the clustering of ectopic cells within the surrounding mesenchyme were observed in the developing rhinencephalon, basal ganglia, thalamus and hippocampal formation in H&E stained sections from all FKRP^{KD} embryos (Figure 1, Figure 2G,H).

Preplate splitting is disturbed in FKRP^{KD} embryos

Detailed histological examination of embryos at E12.5 (Figure 3A-F) revealed multifocal disruption to the basement membrane, associated with disorganisation of the preplate and failure of the preplate to split. These lesions were identified in all FKRP^{KD} embryos at this time point (Figure 1). Neurons were observed herniating through the basement membrane defects, often encompassing subarachnoid vessels, imparting a verrucous appearance at the cortical surface. These lesions were present in multiple locations in the developing brain, including the striatum of the lateral ganglionic eminence, the thalamus and hippocampal formation, but also in the anterior neocortex. Many of the locations correlated with sites at which lesions were obvious at P0. However, some affected areas did not demonstrate obvious neuropathological lesions at P0 (such as the thalamus).

Defects in the pial basement membrane and the glia limitans correlate with both the degree of dyslamination and an absence of glycosylated alpha dystroglycan

Pan laminin immunolabelling showed continuous staining of the pial and vascular basement membranes in wild type embryos at E12.5. In FKRP^{KD} embryos however, there was an extensive disruption of the pial basement membrane (Figure 4A-D). Whilst the vessels were mislocalised (and,

multifocally, almost completely encompassed by ectopic neurons), the vascular basement membranes themselves appeared intact. Immunolabelling for glycosylated alpha dystroglycan (IIH6) was evident both at the basement membrane, and in cellular processes within the ventral thalamus and the cortical hem of wild type embryos. Examination of coronal sections from FKRP^{KD} embryos at this time point confirmed the absence of glycosylated alpha dystroglycan (Figure 4E,F). Beta dystroglycan was however, apparent in both wild type and mutant embryos characterised by granular immunopositive staining of cell bodies in the ventricular zone, which multifocally extended along cell processes. Labelling was particularly prominent in the developing thalamus, at the ganglionic eminences, and ventrally (Figure 5A,B). In addition to this, in wild type embryos, there was continuous laminar staining at the pial basement membrane whereas in the FKRP^{KD} embryos, beta dystroglycan staining at the basement membrane was fragmented. The vascular basement membranes were highlighted in both wild type controls and FKRP^{KD} embryos.

Since the onset of brain lipid binding protein (BLBP) expression coincides with the differentiation of neuroepithelial cells into radial glial cells, this marker was used to confirm that this phenotype preceded the formation of the radial glial scaffold. Indeed at E12.5, both the FKRP^{KD} and wild type exhibited similar patterns of BLBP staining, with foci of immunopositive cells at the medial ganglionic eminences, in the pallium (dorsal to the cortical hem) and in lateral aspects of the developing thalamus, but not at the glia limitans (Figure 5E-H). Overall these observations show that basement membrane defects in FKRP^{KD} mice are first evident very early in development, prior to splitting of the preplate and the formation of the radial glial scaffold, the end feet of which have previously been attributed with a role in stabilising the basement membrane during periods of rapid cortical expansion [32].

Degenerative lesions, and fusion of the interhemispheric fissure, occur late in brain development

Examination of serial-sectioned brains from FKRP^{KD} embryos harvested at E15.5 revealed extensive defects in cortical lamination, with substantial glioneuronal heterotopia present in all of the embryos

examined (Figure 1). Fusion of the interhemispheric fissure and hydrocephalus, reported in FKRP^{KD} mice at P0 [37], were not present at this time point, indicating that these lesions develop later in foetal development. Interestingly, in some areas (particularly the pyriform cortex), disruption appeared more extensive than at P0 suggesting there may be some degree of compensation occurring during the later stages of brain development (Figure 6A-H).

As observed at E10.5 and E12.5, the pial basement membrane in FKRP^{KD} mice at E15.5 was not identifiable with laminin, IIH6 or beta dystroglycan immunolabelling. Laminin immunolabelling revealed that the subarachnoid vessels, which are superficial to the pia mater in the subarachnoid space at the surface of the brain in wild type mice, were partially to totally surrounded by ectopic neurons in FKRP^{KD} embryos (Figure 6I,J). Immunolabelling for the IIH6 epitope of glycosylated alpha dystroglycan delineated the pial basement membrane in wild type embryos but labelling was absent in FKRP^{KD} mice (Figure 6K, L). Beta dystroglycan labelled the blood vessels, the pia and the arachnoid of wild type mice, however in FKRP^{KD} mice, whilst there was some staining of cell bodies in the ventricular zone, of the arachnoid mater and subarachnoid vessels; the pia was not apparent (Figure 6M, N). Levels of staining for beta dystroglycan in the FKRP^{KD} were however, similar to those observed in wild type embryos (Figure 6M, N). BLBP immunolabelling at E15.5 consistently labelled the radial glial cell bodies within the subventricular zone at all levels of the developing CNS. In addition to this, in wild type animals, there was a narrow (approximately 1µm), continuous immunopositive layer, apparent at the peripheral margin of the cortex, consistent with the glia limitans. The glia limitans was not identifiable in FKRP^{KD} mice, although scattered immunopositive foci (representing detached radial glial end feet) were present within the disorganised cortical plate and extra cortical layer (Figure 6O,P).

Cajal-Retzius cells are mislocalised and are morphologically abnormal in FKRP^{KD} mice

We have previously demonstrated a statistically-significant decrease in the number of Cajal-Retzius cells in the rostral cortex of FKRP^{KD} mice at P0, with a concurrent increase in numbers at the level of the hippocampus at this time point [37]. Here, investigation of Cajal-Retzius cells at earlier

developmental time points, revealed mislocalisation at E12.5 (Figure 7A, B) and E15.5 (Figure 7C, D). At E12.5, in wild type animals, the Cajal-Retzius cells formed a monolayer in the superficial preplate (preplate splitting). In the FKRP^{KD}, clusters of reelin-positive cells were located in the caudal neocortex, in the region of the cortical hem and the developing hippocampal formation. By E15.5 Cajal-Retzius cells in FKRP^{KD} mice, rather than forming a discrete layer below the pial basement membrane, were instead surrounded by heterotopic neurons (Figure 7C, D). In agreement with these observations, quantitative analyses showed that in the rostral cortex, numbers of Cajal-Retzius cells in FKRP^{KD} mice were significantly decreased (Figure 7E).

Cell signalling during brain development in FKRP^{KD} mice

There is no discernable perturbation of the reelin signalling pathway in FKRP^{KD} mice at P0

In view of the observed mislocalisation of Cajal-Retzius cells we next sought to determine if signalling pathways downstream of reelin had been disrupted. Disabled-1 (Dab1) is a phosphoprotein, which serves as a reelin signal transducer [39] and complexes with the intracytoplasmic domains of the lipoprotein receptors VLDL and ApoER2, and with the intracytoplasmic domain of α3β1 integrin. Reelin binding to one of these receptors leads to phosphorylation of Dab1, binding of Lis1 and activation of non-receptor tyrosine kinases. In addition, phosphorylated Dab1 becomes polyubiquitinated, targeting it for degradation by the proteasome. This serves as a feedback loop, providing the "stop" signal which prevents neuronal overmigration. *Reeler* mice have been demonstrated to accumulate non-phosphorylated Dab1 in the cortex [39].

Western blot analyses showed Dab1 expression to be similar in both wild type and FKRP^{KD} mice at P0 (Figure 8A). No difference was observed in Dab1 expression in mutant and wild type mice at E15.5 (data not shown). Lis1, also known as platelet-activating factor acetylhydrolase IB subunit alpha (PAFAH1B) is a protein which binds to dynein, regulating microtubule reorganisation within cells. Lis1 is known to be mutated in cases of classical lissencephaly and is downstream in the reelin signalling

pathway [40]. However, Western blot analysis of brain lysates at P0 showed no difference in the amount of Lis1 protein in the brains of FKRP^{KD} mice relative to wild type at P0 (Figure 8B).

There are no downstream changes evident in the phosphatidylinositol 3-kinase (PI3K) signalling pathway

The PI3K/Akt pathway is common intracellular signalling pathway which is downstream of a number of non-receptor tyrosine kinases, G-protein-coupled receptors, B and T cell receptors and others, including lipoprotein and integrin receptors. It is a common downstream component of both β1 integrin and reelin signalling pathways. Stimulation of these leads to production of phosphatidylinositol 3, 4, 5 triphosphates by PI3K, which in turn activate Akt. Activation of this pathway has a diverse range of effects on processes such as cell proliferation and survival (particularly apoptosis), protein synthesis and glucose synthesis. Given the changes observed in reelin expression immunohistochemically, and Lis1 by western blot, we therefore sought to determine if there were any downstream effects on Akt activity. Western blots revealed that expression of Akt was similar in wild type and FKRP^{KD} mice at P0, as were the levels of phosphoAkt (Figure 8A, B). Semi quantitative analyses of these blots is shown in Figure 8C where levels were normalised against beta dystroglycan.

Discussion

Four key events have been previously implicated in the development of cobblestone lissencephaly – neuroglial ectopia (caused by neuronal overmigration), Cajal-Retzius cell mislocalisation, and disruption to the pial basement membrane, with abnormal anchorage of radial glial cells. These factors are considered to be interrelated, but the precise mechanisms underlying their development are unknown.

Dystroglycan is widely expressed and has been attributed with a key role in basement membrane deposition/assembly [41]. The current work shows that that lesions in the basement membrane initially arise between E10.5-E11.5 in FKRP^{KD} mice which is consistent with such a role, but is much earlier than has been reported in other dystroglycanopathy mouse models. Interestingly the only

other mouse model with a cobblestone lissencephaly phenotype currently reported to exhibit brain defects as early as the FKRP^{KD} mouse, is a model with a deletion of the nidogen binding site of laminin γ1 [42]. Similar to FKRP^{KD} mice, this model exhibited breakdown of the basement membrane from E10.5 and failure of migration of the Cajal-Retzius cells [42].

In Pomgnt1$^{-/-}$ mice, Pomt2$^{f/f;Emx1\text{-}Cre+}$ mice and Nestin cre-DG null mice, basement membrane defects and neuroglial ectopia were first observed at E13.5 [38, 43, 44]. E13.5 is a time point at which the developing cortex begins to undergo rapid expansion by the radial migration of post-mitotic neurons. The identification of lesions at this time point therefore led authors to conclude that defects in the ability of radial glial cells to appropriately organise/stabilise the basement membrane during this period of rapid cortical expansion underpinned the neuronal migration defects in these models [32, 44]. Some of the discrepancies with our observations of early defects at E10.5 may however, relate to the precise time point at which expression of either dystroglycan or its glycosylation was removed/altered in this work. In the case of the Pomt2$^{f/f;Emx1\text{-}Cre+}$, whilst Pomt2 expression was knocked-out from approximately E9.5, this was limited to the neural progenitor cells [43]. In Nestin cre-DG null mice, expression of dystroglycan was removed from E10.5, and glycosylated alpha dystroglycan (evident as IIH6 immunoreactivity) present until E12.5 [44]. The mutation in the FKRP^{KD} mouse used in this study is consitituitve. As radial glial cells do not differentiate until around E12.5 in the mouse [45], our observations at E10.5 suggest the involvement of other cellular events and a more complex pathogenesis than originally appreciated in the dystroglycanopathies.

Cajal-Retzius cells migrate between E10.5-E11.5, coinciding with the time point at which brain lesions are first apparent in FKRP^{KD} mice. Indeed, we observed that Cajal-Retzius cells fail to migrate normally in FKRP^{KD} mice, and showed that there are significant decreases in the number of Cajal-Retzius cells in the rostral cortex of FKRP^{KD} mice at E15.5, when compared to wild type controls.

The decrease in the number of Cajal-Retzius cells in the rostral cortex at E15.5, indicated by counts of reelin-positive cells, suggests either a failure of migration of Cajal-Retzius cells or a decrease in the

number of these cells. We have previously identified an increase in the number of Cajal-Retzius cells in neonatal FKRP^{KD} mice at the level of the hippocampus – a structure which develops from the cortical hem (a birth place of Cajal-Retzius cells) [37]. However, Cajal-Retzius cells are a heterogeneous group of cells, with different sites of origin, gene expression patterns and migratory routes [46-48]. The rostral and lateral cortex of mice are populated by Cajal-Retzius cells which originate from the medial septum and the ventral pallium [46, 47]. These data together with that previously reported therefore suggests that a knock down in *Fkrp* specifically affects the subpopulations of Cajal-Retzius cells originating from the medial septum and ventral pallium, whereas those originating from the cortical hem are relatively spared.

Mislocalisation of Cajal-Retzius cells in mouse models of the dystroglycanopathies (including Pomgnt1$^{-/-}$ mice and Nestin cre/DG-null mice) has been identified by others, although the pattern of mislocalisation in these models was not suggestive of failure of migration from their site of origin [32, 38]. Failure of Cajal-Retzius cell migration has been previously reported in mouse models with cobblestone lissencephaly phenotypes not associated with the hypoglycosylation of alpha dystroglycan, namely mice deficient in β2 and γ3 laminins, and those with a deletion of the nidogen binding site of laminin γ1 [42, 49]. These observations together with our data suggest that the migratory route of this cell population is dependent on early basement membrane formation. Whether this dependence is mediated via secreted cues or through direct interaction is not clear at the present time.

Neuroepithelial cells are the precursors of the radial glial cell population. Considering the role of radial glial cells in basement membrane maintenance at later gestational time points [32], and the relatively high expression of the IIH6 epitope of alpha dystroglycan by neuroepithelial cells in wild type mice at early developmental stages, it might be suggested that our observations relate to defects in the neuroepithelial cells. However, Cajal-Retzius cell migration has previously been shown to be independent of the neuroepithelium, and instead dependent on the integrity of the leptomeninges

[33]. The role of the leptomeninges in Cajal-Retzius cell migration, and the disruption to the leptomeninges we have previously reported in FKRP^{KD} mice at P0, focuses attention on a potential role for these cells in the pathogenesis of the brain phenotype in FKRP^{KD} mice [37].

In spite of a significant decrease in the number of Cajal-Retzius cells in the rostral cortex of FKRP^{KD} mice at P0, no global changes were observed in Lis1, Dab1 or Akt (Figure 8) which are all components of the reelin signalling pathway [50]. Mutations in *LIS1* and *RELN,* which result in a decrease or loss of expression of these proteins, have previously been identified as causes of classical (type I) lissencephaly [51, 52], but expression of Lis1 has not previously been investigated in the cobblestone lissencephalies. Our data shows the cell autonomous nature of this signalling pathway and moreover, indicates that an early event in the disease process is due to mislocalisation of reelin rather than an alteration in downstream signalling processes. Interestingly beta dystroglycan showed a small reduction in the FKRP^{KD} relative to wild type. As to whether this is a secondary consequence of basement membrane disruption or reflects a down regulation of the Dag1 gene is unclear at the present time.

Conclusions

In summary, our work shows that basement membrane defects predate radial glial cell differentiation and occur around the time of Cajal-Retzius cell migration. In agreement with this Cajal-Retzius cells are mislocalised from early in brain development, however, this was not associated with any apparent disruption in the reelin, and downstream PI3K/Akt signalling pathways.

Acknowledgements: HSB and SCB designed the study and wrote the paper, HSB, VPV, JLW and MH performed the experiments and analysed the data. The authors gratefully acknowledge financial support from the Royal Veterinary College and confirm that they have no conflict of interests either personally or financially.

Figure legends.

Figure 1: Incidence of brain lesions in FKRP^{KD} mice

A. Incidence of brain lesions in FKRP^{KD} embryos. Evidence of a neuronal migration defect, manifest as neuroglial heterotopia, was apparent in 60% of all FKRP^{KD} embryos at E10.5. At later developmental time points, these lesions were identified in 100% of FKRP^{KD} embryos. B – E. Semi-quantitative ranking of the severity of lesions in FKRP^{KD} embryos. Lesions were initially subtle and focal in nature, but through development became much more substantial and were multifocal to coalescing. There was some variation in the severity of brain lesions in FKRP^{KD} mice from E11.5 onwards. Lesion severity was ranked as follows: 0 = normal, 1 = minimal. Focal defect in the pial basement membrane, with herniation of cells through the defects, 2 = mild. Multifocal defects in the PBM, herniation of cells through defects. 3 = moderate. Moderate disorganisation of the developing cortex, limited or multifocal organisation of the cortical plate. 4 = marked. Significant disruption to the developing cortex, no differentiation of the areas of organisation. 5 = massive. Complete disorganisation of the developing cortex, no normal structures apparent.

A

Gestational age	Genotype	
	Wild type	FKRP^{KD}
E10.5	0/5	3/5
E11.5	0/4	4/4
E12.5	0/4	6/6
E15.5	0/5	5/5

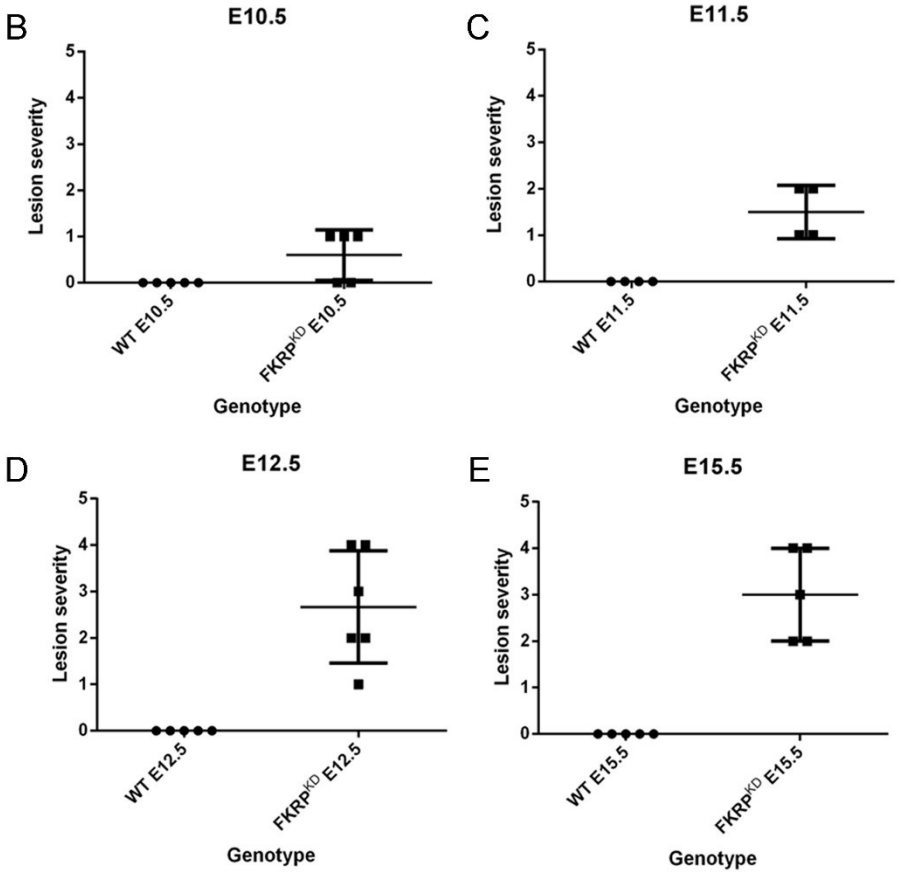

Figure 2: Early brain development in FKRP^{KD} mice

A, B. Subtle lesions, characterised by multifocal disorganisation of the neuroepithelium, are apparent in the striatum of the LGE in HE stained sections of 60% of FKRP^{KD} embryos at E10.5 (arrowheads). C, D. Immunolabelling of the IIH6 epitope of glycosylated alpha dystroglycan at E10.5 reveals there is strong, diffuse staining of the wild type neuroepithelium at this time point (C). In addition, note the strong staining of the adjacent developing oral epithelium. Immunolabelling is not present in the FKRP^{KD} (D). E, F. Laminin immunolabelling. In wild type mice, a continuous, laminar, immunopositive layer is present along the surface of the neuroepithelium (basement membrane), although the neuroepithelium itself does not stain. There is some staining of the adjacent, as yet undifferentiated mesenchyme. In contrast to the neuroepithelium, the oral epithelium is strongly immunopositive. In the FKRP^{KD} mice at this time point, an immunopositive neuroepithelial basement membrane is not apparent. G, H. By E11.5, brain lesions, characterised by disorganisation of the neuroepithelium and clustering of ectopic cells within the surrounding mesenchyme, are obvious in the HE stained sections of all FKRP^{KD} mice examined (arrowheads). A, B, G, H – bars represent 100µm; C, D, E, F – bars represent 50µm. NE = neuroepithelium; M = mesenchyme; BV = blood vessels; OE = oral epithelium; LGE = lateral ganglionic eminence.

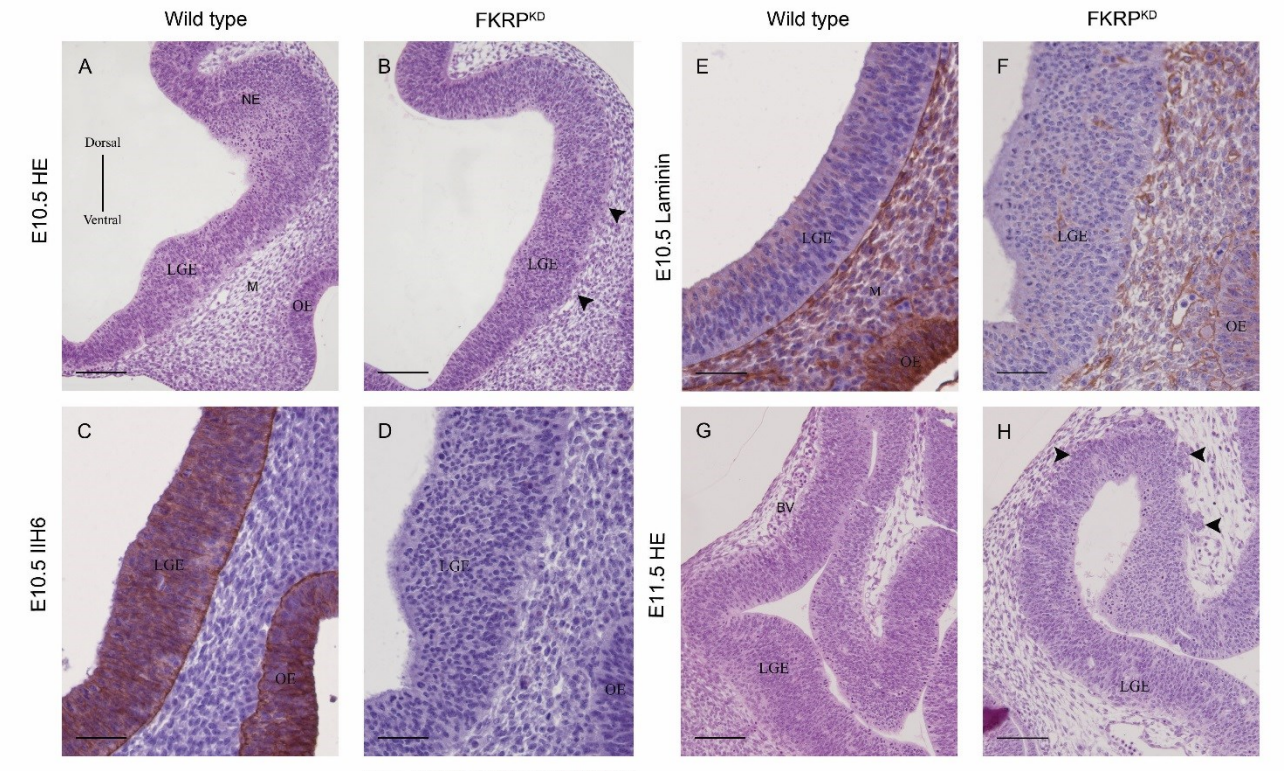

Figure 3: FKRP^{KD} at the preplate stage

A, B. Cortex (cortical hem). The cortex, intermediate zone of the lateral ganglionic eminence and thalamus are disrupted in FKRP^{KD} mice at this level (bold arrows). C, D. The intermediate thalamus, temporal cortex and occipital cortex demonstrate disorganisation and cell ectopia in FKRP^{KD} mice (bold arrows). E, F. In wild type mice, the developing cortex is organised and the pial basement membrane is visible (arrow heads). Disorganisation of the preplate and cluster of ectopic cells are readily apparent in the FKRP^{KD} at this time point (bold arrows). HE. MS = medial septum; LGE = lateral ganglionic eminence; C = Cortex; T = thalamus; CH = cortical hem; MGE = medial ganglionic eminence; H = hippocampus. A-D bars represent 200µm E-F bars represent 100µm

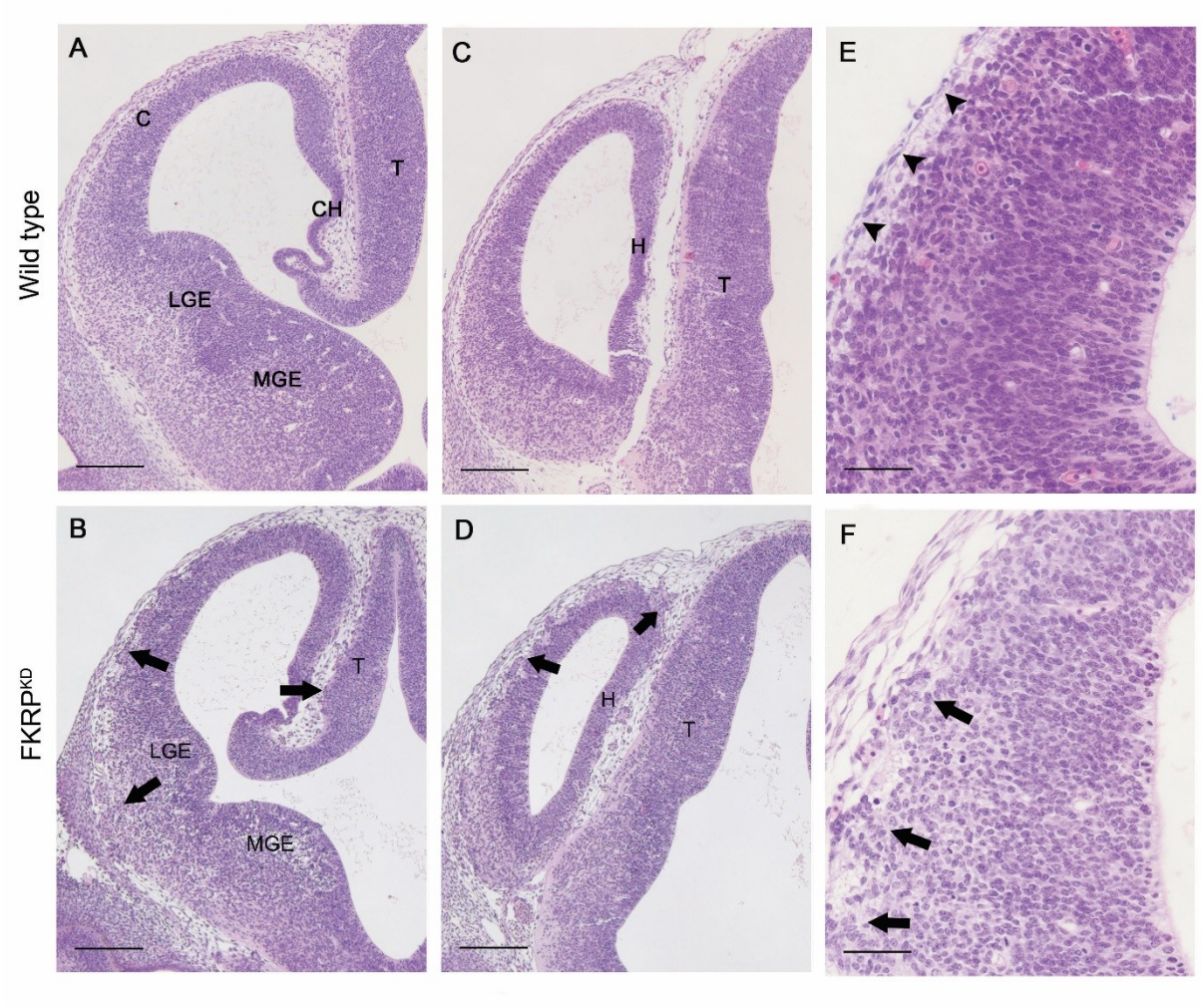

Figure 4: FKRP^{KD} at the preplate stage

A-D. Laminin immunolabelling. In wild type mice, a continuous, laminar, immunopositive layer is present along the surface of the preplate (basement membrane), similar to that observed at E10.5 (arrowheads). Laminin staining is visible within the developing brain in areas which ultimately differentiate into the choroid plexus and the dorsal thalamus. Basement membrane staining at the surface of the preplate is not apparent in FKRP^{KD} mice, but is retained at the choroid plexus and the dorsal thalamus. E, F. Immunolabelling for the IIH6 epitope of glycosylated alpha dystroglycan. A continuous, laminar immunopositive layer is present along the surface of the preplate (basement membrane) in wild type embryos (arrowheads). In addition, there is intense staining of cell bodies and processes, particularly in the thalamus and at the cortical hem (star). Immunolabelling is not present in developing brains of the FKRP^{KD} embryos. C = Cortex; MS = medial septum; LGE = lateral ganglionic eminence; T = thalamus; CH = cortical hem; MGE = medial ganglionic eminence. A, B, E, F – bars represent 100µm. C,D – bars present 50µm.

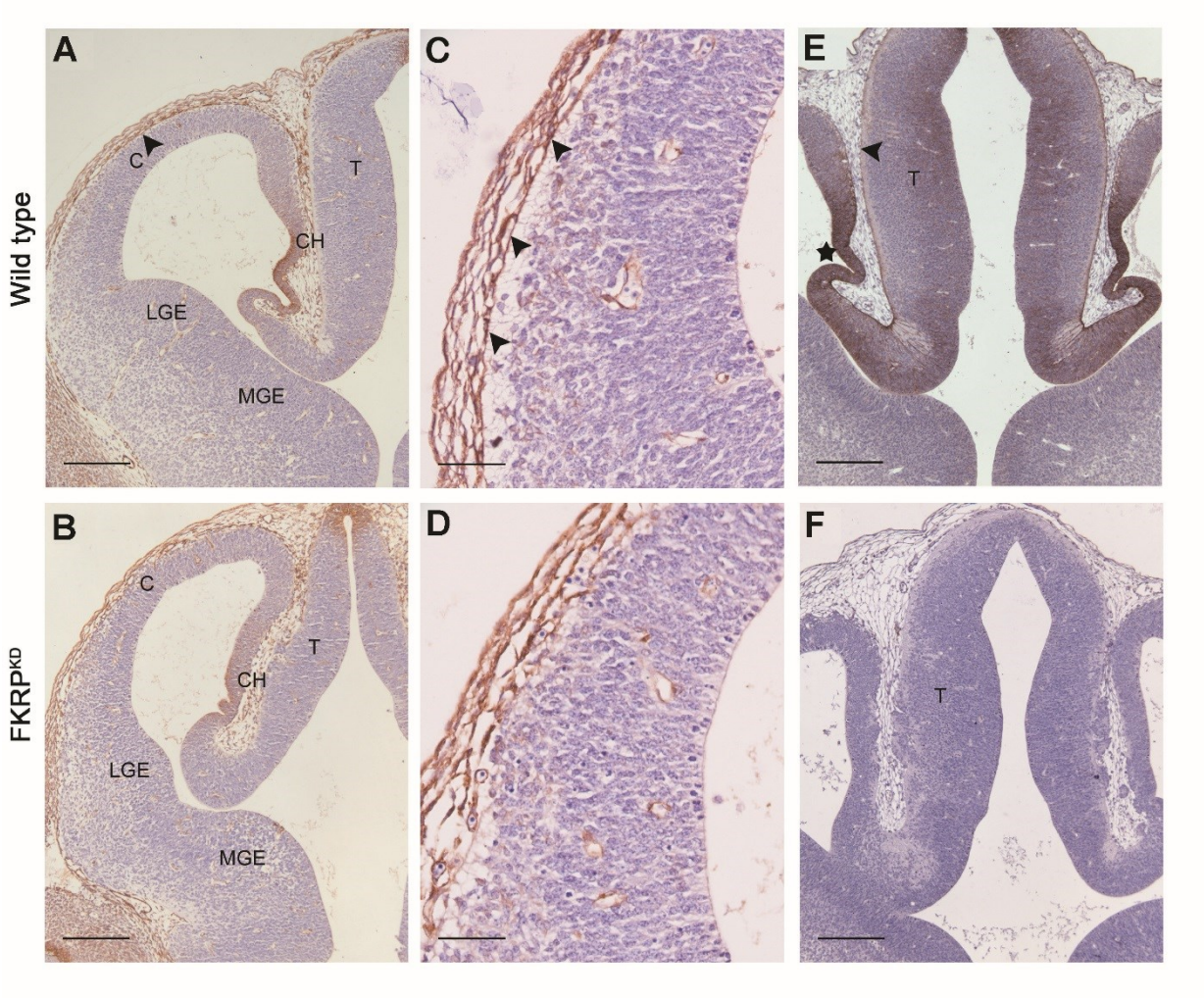

Figure 5: FKRP^{KD} at the preplate stage

A-D. Beta dystroglycan immunolabelling. Immunostaining in wild type and FKRP^{KD} embryos is similar, with beta dystroglycan expression at the basement membrane of the preplate (arrowheads) and the choroid plexus, in addition to being present in cell bodies in the ventricular zone and extending along cell processes. In FKRP^{KD} embryos, there are defects in the laminar staining of the basement membrane of the preplate, most obviously in the thalamus (*), shown at the higher magnification in (D), but also extensively in lateral aspects of the cortex and the LGE. E-H. BLBP immunolabelling. There is immunolabelling of cell bodies in the ventricular zone, along with the glia limitans and some cell processes in the thalamus. In the cortex, the glia limitans does not stain diffusely with BLBP at this time point in either wild type of FKRP^{KD} embryos, suggesting that this is the developmental point at which differentiation from neuroepithelial cells to radial glial cells is beginning. LGE = lateral ganglionic eminence; T = thalamus; CH = cortical hem. A-F bars represent 200µm. G, H bars represent 50µm.

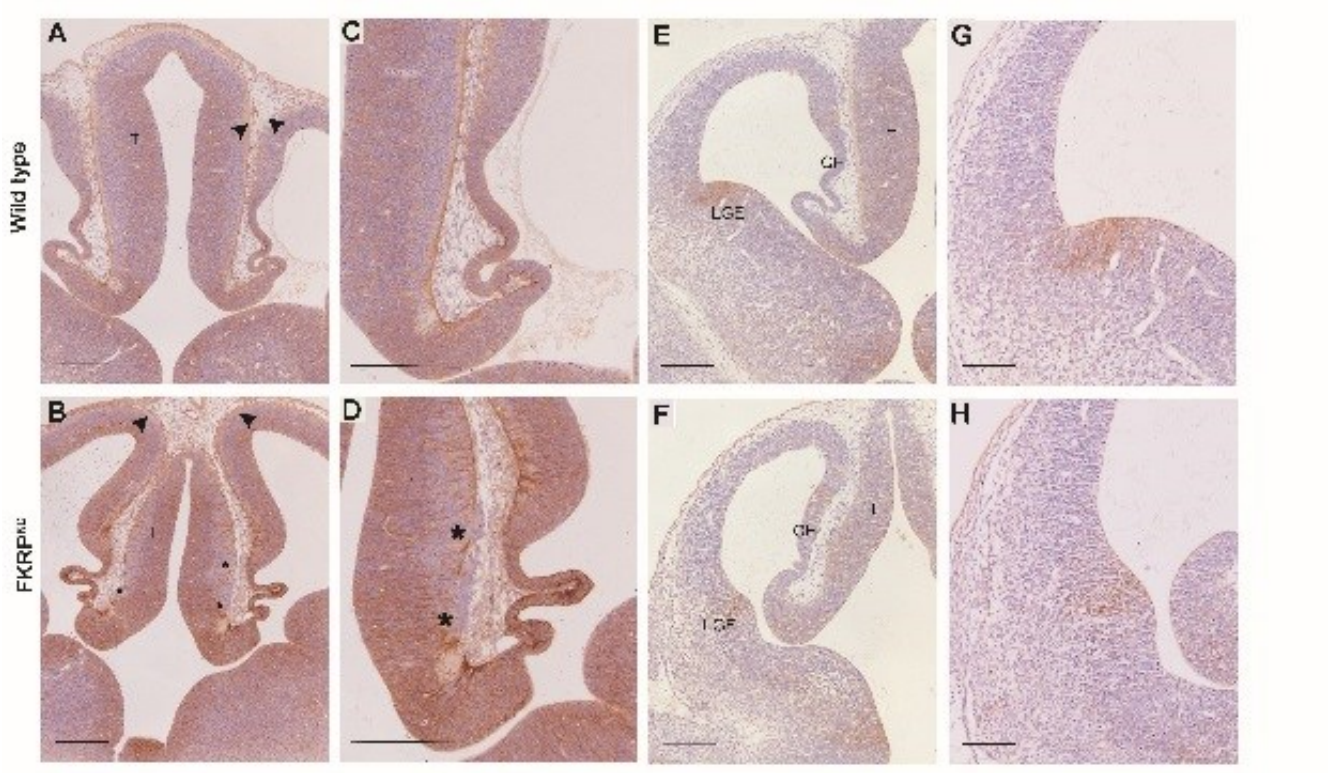

Figure 6: FKRP^{KD} brain during rapid cortical expansion

A-D The cortical hemispheres remain distinct in the FKRP^{KD} at this time point, although laminar organisation is largely absent, and both the cortical plate and the marginal zone are inapparent. The cortical surface has a marked, irregular appearance, which extends laterally (B,D see arrows). Ventrally and caudolaterally, the striatum and pyriform lobes appear decreased in size when compared to wild type mice at this time point. E, F. The FKRP^{KD} exhibits disorganisation of the inferior colliculus. I, J. A higher magnification view of the neocortex in wild type and FKRP^{KD} mice. In FKRP^{KD} mice there is marked disruption to the cortical plate (bold arrows) and the marginal zone is inapparent. Normally superficial blood vessels are multifocally surrounded by ectopic cells. HE. A - F bars represent 400µm; G, H bars represent 100µm. I, J. Laminin. Immunolabelling reveals marked disruption to the pial basement membrane in FKRP^{KD} mice. The subarachnoid vessels, normally apparent superficial to the pia at the surface of the brain are partially to totally surrounded by ectopic neurons. Arrowhead indicated normal staining of the basement membrane in wild type mice. Inserts show the presence and altered distribution of laminin in the wild type and FKRP^{KD} respectively. K, L. Immunolabelling for the IIH6 epitope of glycosylated alpha dystroglycan. Pial basement membranes (arrowhead) are strongly immunopositive in wild type mice. Staining is not present in the FKRP^{KD} mice. M, N. Beta dystroglycan. Blood vessels, the pia (arrowhead) and the arachnoid (fine arrow) are immunopositive in wild type mice. There is some staining of cell bodies in the ventricular zone. In the FKRP^{KD}, immunolabelling of arachnoid and subarachnoid vessels (surrounded by ectopic neurons) are still apparent, but the pia is not observed. Inserts show higher magnification of the cortical surface. O, P. BLBP. In addition to staining at the ventricular zone, there is continuous, laminar staining of the glia limitans in wild type mice (bold arrow). Scattered BLBP-positive foci are present in the FKRP^{KD} (bold arrow). M = motor cortex; I = insular cortex; P = pyriform lobe; H = hippocampus; LGE = lateral ganglionic eminence; Cb = cerebellum; SC = superior colliculus; MZ = marginal zone; CP = cortical plate; SP = subplate; IZ = intermediate zone; VZ = ventricular zone.

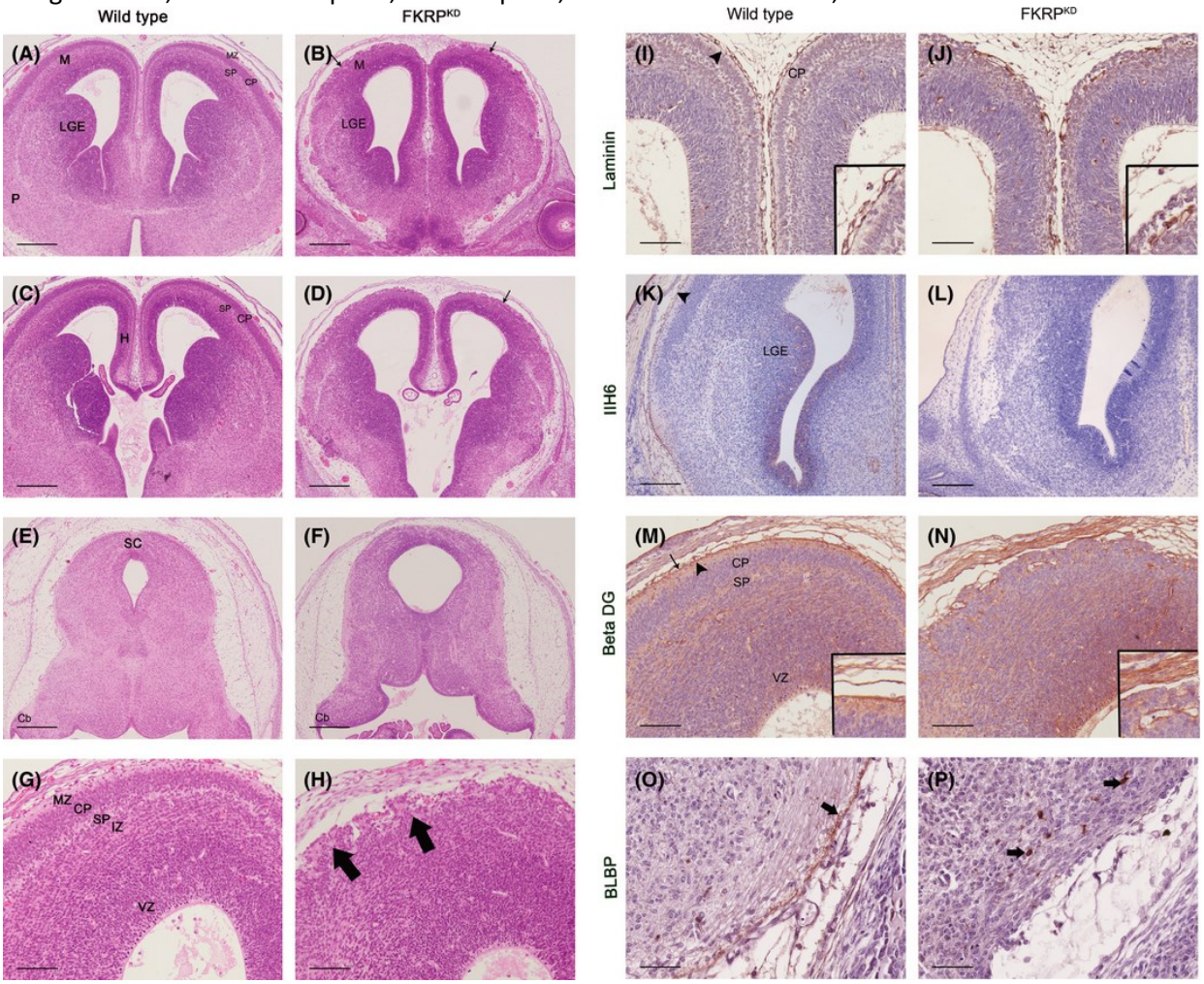

Figure 7: Localisation of Cajal-Retzius cells through brain development

Immunohistochemical staining with antibodies to reelin. Cajal-Retzius cells are mislocalised early in brain development and prior to the differentiation of radial glial cells. A, B. At E12.5, in the FKRP^{KD}, Cajal-Retzius cells are mislocalised, often clustered in the mesenchyme surrounding the developing brain. C, D. By E15.5, in the dorsolateral cortex of FKRP^{KD} mice, numbers of Cajal-Retzius cells (bold arrows) appear dramatically reduced. Rather than forming a discrete layer below the pial basement membrane (arrowheads) within the marginal zone as in wild type mice, Cajal-Retzius cells are surrounded by heterotopic neurons. E. In the rostral cortex at E15.5, there was a statistically significant decrease in the number of Cajal-Retzius cells in FKRP^{KD} mice when compared with wild type controls (unpaired t test with Welch's correction, P = 0.0053). A – D bars represent 100µm.

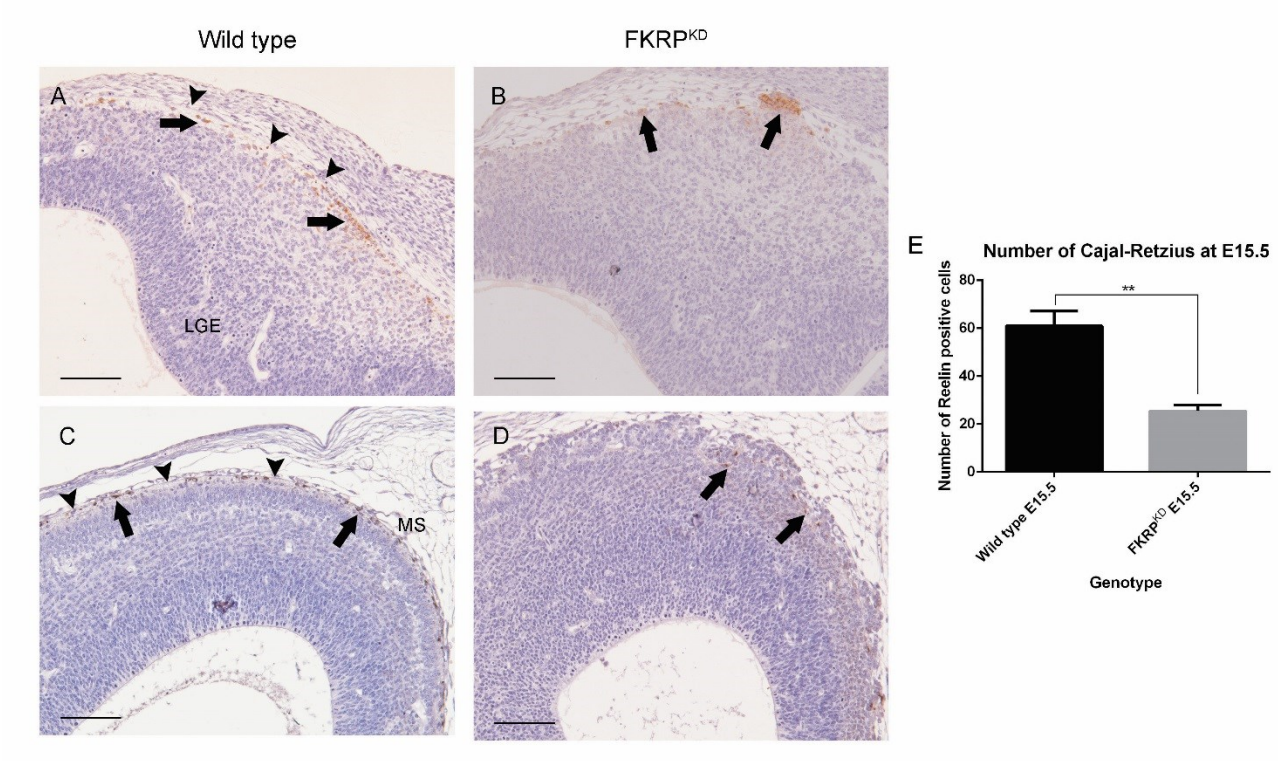

Figure 8: Reelin signalling in the brain at P0

An analysis of whole brain extracts at P0 from wild type and FKRP^{KD} (mutant) mice. A. DAB1 and Akt, B. phospho Akt, Lis1 and beta dystroglycan C. a semi quantitative assessment of levels using densitometry. All levels were normalised to the loading control (beta dystroglycan) and indicate no statistically significant differences (two sample t-test) between wild type and FKRP^{KD} with respect to either DAB1, Akt, phospho Akt or Lis 1. Error bars represent standard error of the mean. No alteration in the mobility of beta dystroglycan is evident in the FKRP^{KD} compared to wild type.

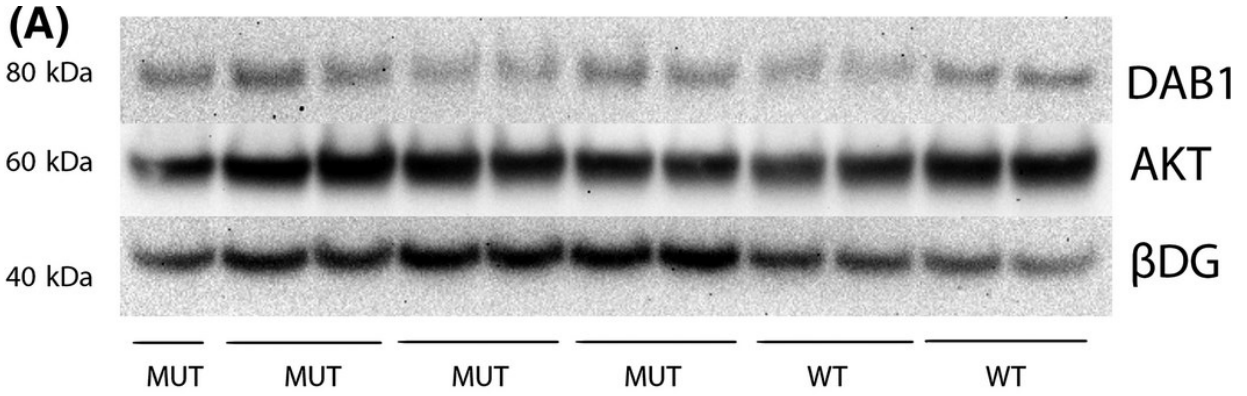

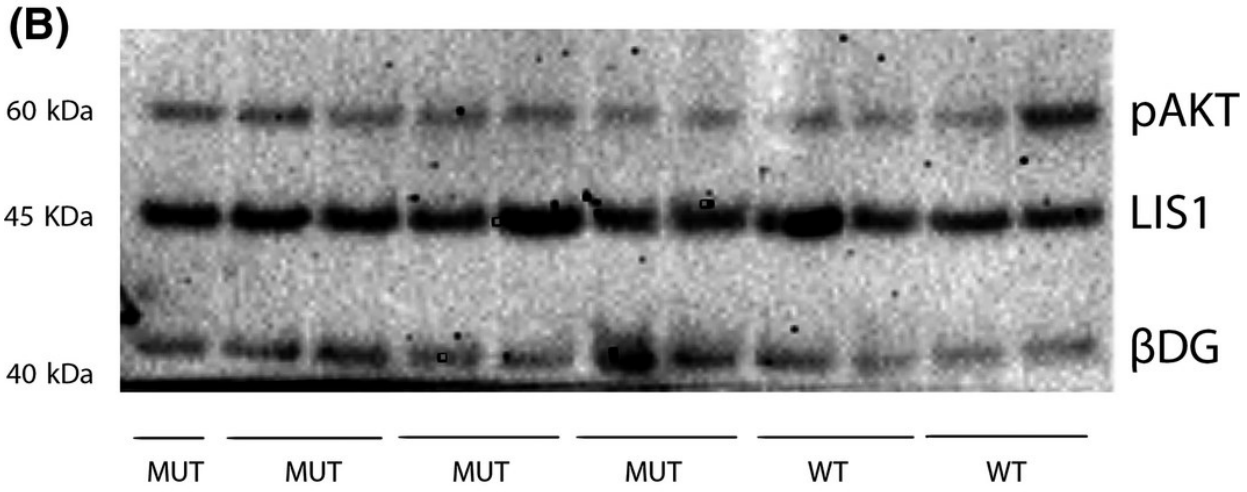

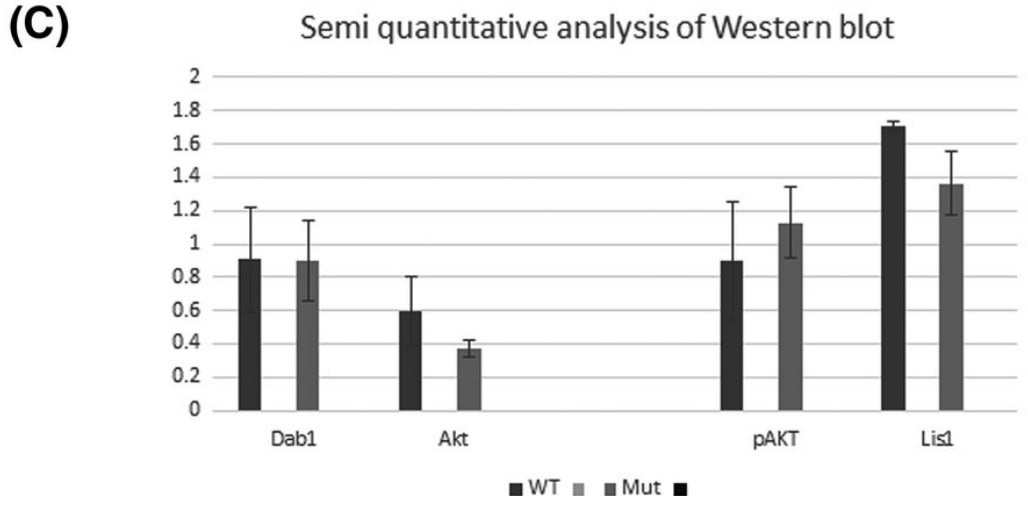

References

1 Dobyns WB, Kirkpatrick JB, Hittner HM, Roberts RM, Kretzer FL. Syndromes with lissencephaly. II: Walker-Warburg and cerebro-oculo-muscular syndromes and a new syndrome with type II lissencephaly. Am J Med Genet 1985; 22: 157-95

2 Bouchet C, Gonzales M, Vuillaumier-Barrot S, Devisme L, Lebizec C, Alanio E, Bazin A, Bessieres-Grattagliano B, Bigi N, Blanchet P, Bonneau D, Bonnieres M, Carles D, Delahaye S, Fallet-Bianco C, Figarella-Branger D, Gaillard D, Gasser B, Guimiot F, Joubert M, Laurent N, Liprandi A, Loget P, Marcorelles P, Martinovic J, Menez F, Patrier S, Pelluard-Nehme F, Perez MJ, Rouleau-Dubois C, Triau S, Laquerriere A, Encha-Razavi F, Seta N. Molecular heterogeneity in fetal forms of type II lissencephaly. Human mutation 2007; 28: 1020-7

3 Devisme L, Bouchet C, Gonzales M, Alanio E, Bazin A, Bessieres B, Bigi N, Blanchet P, Bonneau D, Bonnieres M, Bucourt M, Carles D, Clarisse B, Delahaye S, Fallet-Bianco C, Figarella-Branger D, Gaillard D, Gasser B, Delezoide AL, Guimiot F, Joubert M, Laurent N, Laquerriere A, Liprandi A, Loget P, Marcorelles P, Martinovic J, Menez F, Patrier S, Pelluard F, Perez MJ, Rouleau C, Triau S, Attie-Bitach T, Vuillaumier-Barrot S, Seta N, Encha-Razavi F. Cobblestone lissencephaly: neuropathological subtypes and correlations with genes of dystroglycanopathies. Brain 2012; 135: 469-82

4 Ervasti JM, Campbell KP. A role for the dystrophin-glycoprotein complex as a transmembrane linker between laminin and actin. The Journal of cell biology 1993; 122: 809-23

5 Yoshida A, Kobayashi K, Manya H, Taniguchi K, Kano H, Mizuno M, Inazu T, Mitsuhashi H, Takahashi S, Takeuchi M, Herrmann R, Straub V, Talim B, Voit T, Topaloglu H, Toda T, Endo T. Muscular dystrophy and neuronal migration disorder caused by mutations in a glycosyltransferase, POMGnT1. Developmental cell 2001; 1: 717-24

6 Yeo LY, Matar OK, Perez de Ortiz ES, Hewitt GF. Simulation studies of phase inversion in agitated vessels using a Monte Carlo technique. J Colloid Interface Sci 2002; 248: 443-54

7 Gee SH, Montanaro F, Lindenbaum MH, Carbonetto S. Dystroglycan-alpha, a dystrophin-associated glycoprotein, is a functional agrin receptor. Cell 1994; 77: 675-86

8 Moore CJ, Winder SJ. Dystroglycan versatility in cell adhesion: a tale of multiple motifs. Cell communication and signaling : CCS 2010; 8: 3

9 Sugita S, Saito F, Tang J, Satz J, Campbell K, Sudhof TC. A stoichiometric complex of neurexins and dystroglycan in brain. The Journal of cell biology 2001; 154: 435-45

10 Beltran-Valero de Bernabe D, Currier S, Steinbrecher A, Celli J, van Beusekom E, van der Zwaag B, Kayserili H, Merlini L, Chitayat D, Dobyns WB, Cormand B, Lehesjoki AE, Cruces J, Voit T, Walsh CA, van Bokhoven H, Brunner HG. Mutations in the O-mannosyltransferase gene POMT1 give rise to the severe neuronal migration disorder Walker-Warburg syndrome. American journal of human genetics 2002; 71: 1033-43

11 van Reeuwijk J, Janssen M, van den Elzen C, Beltran-Valero de Bernabe D, Sabatelli P, Merlini L, Boon M, Scheffer H, Brockington M, Muntoni F, Huynen MA, Verrips A, Walsh CA, Barth PG, Brunner HG, van Bokhoven H. POMT2 mutations cause alpha-dystroglycan hypoglycosylation and Walker-Warburg syndrome. Journal of medical genetics 2005; 42: 907-12

12 Longman C, Brockington M, Torelli S, Jimenez-Mallebrera C, Kennedy C, Khalil N, Feng L, Saran RK, Voit T, Merlini L, Sewry CA, Brown SC, Muntoni F. Mutations in the human LARGE gene cause MDC1D, a novel form of congenital muscular dystrophy with severe mental retardation and abnormal glycosylation of alpha-dystroglycan. Hum Mol Genet 2003; 12: 2853-61

13 Toda T. [Fukutin, a novel protein product responsible for Fukuyama-type congenital muscular dystrophy]. Seikagaku 1999; 71: 55-61

14 Brockington M, Blake DJ, Prandini P, Brown SC, Torelli S, Benson MA, Ponting CP, Estournet B, Romero NB, Mercuri E, Voit T, Sewry CA, Guicheney P, Muntoni F. Mutations in the fukutin-related protein gene (FKRP) cause a form of congenital muscular dystrophy with secondary laminin alpha2 deficiency and abnormal glycosylation of alpha-dystroglycan. American journal of human genetics 2001; 69: 1198-209

15 Willer T, Lee H, Lommel M, Yoshida-Moriguchi T, de Bernabe DB, Venzke D, Cirak S, Schachter H, Vajsar J, Voit T, Muntoni F, Loder AS, Dobyns WB, Winder TL, Strahl S, Mathews KD, Nelson SF, Moore SA, Campbell KP. ISPD loss-of-function mutations disrupt dystroglycan O-mannosylation and cause Walker-Warburg syndrome. Nature genetics 2012:

16 Roscioli T, Kamsteeg EJ, Buysse K, Maystadt I, van Reeuwijk J, van den Elzen C, van Beusekom E, Riemersma M, Pfundt R, Vissers LE, Schraders M, Altunoglu U, Buckley MF, Brunner HG, Grisart B, Zhou H, Veltman JA, Gilissen C, Mancini GM, Delree P, Willemsen MA, Ramadza DP, Chitayat D, Bennett C, Sheridan E, Peeters EA, Tan-Sindhunata GM, de Die-Smulders CE, Devriendt K, Kayserili H, El-Hashash OA, Stemple DL, Lefeber DJ, Lin YY, van Bokhoven H. Mutations in ISPD cause Walker-Warburg syndrome and defective glycosylation of alpha-dystroglycan. Nature genetics 2012:

17 Yang AC, Ng BG, Moore SA, Rush J, Waechter CJ, Raymond KM, Willer T, Campbell KP, Freeze HH, Mehta L. Congenital disorder of glycosylation due to DPM1 mutations presenting with dystroglycanopathy-type congenital muscular dystrophy. Molecular genetics and metabolism 2013; 110: 345-51

18 Barone R, Aiello C, Race V, Morava E, Foulquier F, Riemersma M, Passarelli C, Concolino D, Carella M, Santorelli F, Vleugels W, Mercuri E, Garozzo D, Sturiale L, Messina S, Jaeken J, Fiumara A, Wevers RA, Bertini E, Matthijs G, Lefeber DJ. DPM2-CDG: a muscular dystrophy-dystroglycanopathy syndrome with severe epilepsy. Annals of neurology 2012; 72: 550-8

19 Lefeber DJ, Schonberger J, Morava E, Guillard M, Huyben KM, Verrijp K, Grafakou O, Evangeliou A, Preijers FW, Manta P, Yildiz J, Grunewald S, Spilioti M, van den Elzen C, Klein D, Hess D, Ashida H, Hofsteenge J, Maeda Y, van den Heuvel L, Lammens M, Lehle L, Wevers RA. Deficiency of Dol-P-Man synthase subunit DPM3 bridges the congenital disorders of glycosylation with the dystroglycanopathies. American journal of human genetics 2009; 85: 76-86

20 Yoshida-Moriguchi T, Willer T, Anderson ME, Venzke D, Whyte T, Muntoni F, Lee H, Nelson SF, Yu L, Campbell KP. SGK196 is a glycosylation-specific O-mannose kinase required for dystroglycan function. Science 2013; 341: 896-9

21 Carss KJ, Stevens E, Foley AR, Cirak S, Riemersma M, Torelli S, Hoischen A, Willer T, van Scherpenzeel M, Moore SA, Messina S, Bertini E, Bonnemann CG, Abdenur JE, Grosmann CM, Kesari A, Punetha J, Quinlivan R, Waddell LB, Young HK, Wraige E, Yau S, Brodd L, Feng L, Sewry C, MacArthur DG, North KN, Hoffman E, Stemple DL, Hurles ME, van Bokhoven H, Campbell KP, Lefeber DJ, Consortium UK, Lin YY, Muntoni F. Mutations in GDP-mannose pyrophosphorylase B cause congenital and limb-girdle muscular dystrophies associated with hypoglycosylation of alpha-dystroglycan. Am J Hum Genet 2013; 93: 29-41

22 Stevens E, Carss KJ, Cirak S, Foley AR, Torelli S, Willer T, Tambunan DE, Yau S, Brodd L, Sewry CA, Feng L, Haliloglu G, Orhan D, Dobyns WB, Enns GM, Manning M, Krause A, Salih MA, Walsh CA, Hurles M, Campbell KP, Manzini MC, Consortium UK, Stemple D, Lin YY, Muntoni F. Mutations in B3GALNT2 cause congenital muscular dystrophy and hypoglycosylation of alpha-dystroglycan. Am J Hum Genet 2013; 92: 354-65

23 Manzini MC, Tambunan DE, Hill RS, Yu TW, Maynard TM, Heinzen EL, Shianna KV, Stevens CR, Partlow JN, Barry BJ, Rodriguez J, Gupta VA, Al-Qudah AK, Eyaid WM, Friedman JM, Salih MA, Clark R, Moroni I, Mora M, Beggs AH, Gabriel SB, Walsh CA. Exome sequencing and functional validation in zebrafish identify GTDC2 mutations as a cause of Walker-Warburg syndrome. American journal of human genetics 2012; 91: 541-7

24 Vuillaumier-Barrot S, Bouchet-Seraphin C, Chelbi M, Devisme L, Quentin S, Gazal S, Laquerriere A, Fallet-Bianco C, Loget P, Odent S, Carles D, Bazin A, Aziza J, Clemenson A, Guimiot F, Bonniere M, Monnot S, Bole-Feysot C, Bernard JP, Loeuillet L, Gonzales M, Socha K, Grandchamp B, Attie-Bitach T, Encha-Razavi F, Seta N. Identification of mutations in TMEM5 and ISPD as a cause of severe cobblestone lissencephaly. Am J Hum Genet 2012; 91: 1135-43

25 Buysse K, Riemersma M, Powell G, van Reeuwijk J, Chitayat D, Roscioli T, Kamsteeg EJ, van den Elzen C, van Beusekom E, Blaser S, Babul-Hirji R, Halliday W, Wright GJ, Stemple DL, Lin YY, Lefeber DJ,

van Bokhoven H. Missense mutations in beta-1,3-N-acetylglucosaminyltransferase 1 (B3GNT1) cause Walker-Warburg syndrome. Hum Mol Genet 2013; 22: 1746-54
26 Shaheen R, Faqeih E, Ansari S, Alkuraya FS. A truncating mutation in B3GNT1 causes severe Walker-Warburg syndrome. Neurogenetics 2013; 14: 243-5
27 Kranz C, Jungeblut C, Denecke J, Erlekotte A, Sohlbach C, Debus V, Kehl HG, Harms E, Reith A, Reichel S, Grobe H, Hammersen G, Schwarzer U, Marquardt T. A defect in dolichol phosphate biosynthesis causes a new inherited disorder with death in early infancy. American journal of human genetics 2007; 80: 433-40
28 Lefeber DJ, de Brouwer AP, Morava E, Riemersma M, Schuurs-Hoeijmakers JH, Absmanner B, Verrijp K, van den Akker WM, Huijben K, Steenbergen G, van Reeuwijk J, Jozwiak A, Zucker N, Lorber A, Lammens M, Knopf C, van Bokhoven H, Grunewald S, Lehle L, Kapusta L, Mandel H, Wevers RA. Autosomal recessive dilated cardiomyopathy due to DOLK mutations results from abnormal dystroglycan O-mannosylation. PLoS genetics 2011; 7: e1002427
29 Ackroyd MR, Skordis L, Kaluarachchi M, Godwin J, Prior S, Fidanboylu M, Piercy RJ, Muntoni F, Brown SC. Reduced expression of fukutin related protein in mice results in a model for fukutin related protein associated muscular dystrophies. Brain 2009; 132: 439-51
30 Ackroyd MR, Whitmore C, Prior S, Kaluarachchi M, Nikolic M, Mayer U, Muntoni F, Brown SC. Fukutin-Related Protein Alters the Deposition of Laminin in the Eye and Brain. The Journal of Neuroscience 2011; 31: 12927-35
31 Moore SA, Saito F, Chen J, Michele DE, Henry MD, Messing A, Cohn RD, Ross-Barta SE, Westra S, Williamson RA, Hoshi T, Campbell KP. Deletion of brain dystroglycan recapitulates aspects of congenital muscular dystrophy. Nature 2002; 418: 422-5
32 Myshrall TD, Moore SA, Ostendorf AP, Satz JS, Kowalczyk T, Nguyen H, Daza RA, Lau C, Campbell KP, Hevner RF. Dystroglycan on Radial Glia End Feet Is Required for Pial Basement Membrane Integrity and Columnar Organization of the Developing Cerebral Cortex. J Neuropathol Exp Neurol 2012:
33 Borrell V, Marin O. Meninges control tangential migration of hem-derived Cajal-Retzius cells via CXCL12/CXCR4 signaling. Nature neuroscience 2006; 9: 1284-93
34 Montagnani S, Castaldo C, Di Meglio F, Sciorio S, Giordano-Lanza G. Extra cellular matrix features in human meninges. Italian journal of anatomy and embryology = Archivio italiano di anatomia ed embriologia 2000; 105: 167-77
35 Copp AJ, Carvalho R, Wallace A, Sorokin L, Sasaki T, Greene ND, Ybot-Gonzalez P. Regional differences in the expression of laminin isoforms during mouse neural tube development. Matrix biology : journal of the International Society for Matrix Biology 2011; 30: 301-9
36 Siegenthaler JA, Ashique AM, Zarbalis K, Patterson KP, Hecht JH, Kane MA, Folias AE, Choe Y, May SR, Kume T, Napoli JL, Peterson AS, Pleasure SJ. Retinoic acid from the meninges regulates cortical neuron generation. Cell 2009; 139: 597-609
37 Booler HS, Williams JL, Hopkinson M, Brown SC. Degree of Cajal-Retzius Cell Mislocalization Correlates with the Severity of Structural Brain Defects in Mouse Models of Dystroglycanopathy. Brain Pathol 2015:
38 Hu H, Yang Y, Eade A, Xiong YF, Qi Y. Breaches of the Pial Basement Membrane and Disappearance of the Glia Limitans During Development Underlie the Cortical Lamination Defect in the Mouse Model of Muscle-Eye-Brain Disease. The Journal of Comparative Neurology 2007; 501: 168-83
39 Rice DS, Sheldon M, D'Arcangelo G, Nakajima K, Goldowitz D, Curran T. Disabled-1 acts downstream of Reelin in a signaling pathway that controls laminar organization in the mammalian brain. Development 1998; 125: 3719-29
40 Reiner O, Carrozzo R, Shen Y, Wehnert M, Faustinella F, Dobyns WB, Caskey CT, Ledbetter DH. Isolation of a Miller-Dieker lissencephaly gene containing G protein beta-subunit-like repeats. Nature 1993; 364: 717-21

41 Yurchenco PD, Cheng YS, Campbell K, Li S. Loss of basement membrane, receptor and cytoskeletal lattices in a laminin-deficient muscular dystrophy. Journal of cell science 2004; 117: 735-42
42 Halfter W, Dong S, Yip YP, Willem M, Mayer U. A critical function of the pial basement membrane in cortical histogenesis. The Journal of neuroscience : the official journal of the Society for Neuroscience 2002; 22: 6029-40
43 Hu H, Li J, Gagen CS, Gray NW, Zhang Z, Qi Y, Zhang P. Conditional knockout of protein O-mannosyltransferase 2 reveals tissue-specific roles of O-mannosyl glycosylation in brain development. J Comp Neurol 2011; 519: 1320-37
44 Satz JS, Ostendorf AP, Hou S, Turner A, Kusano H, Lee JC, Turk R, Nguyen H, Ross-Barta SE, Westra S, Hoshi T, Moore SA, Campbell KP. Distinct Functions of Glial and Neuronal Dystroglycan in the Developing and Adult Mouse Brain. The Journal of Neuroscience 2010; 30: 14560 –72
45 Hartfuss E, Galli R, Heins N, Gotz M. Characterization of CNS precursor subtypes and radial glia. Dev Biol 2001; 229: 15-30
46 Bielle F, Griveau A, Narboux-Neme N, Vigneau S, Sigrist M, Arber S, Wassef M, Pierani A. Multiple origins of Cajal-Retzius cells at the borders of the developing pallium. Nature neuroscience 2005; 8: 1002-12
47 Takiguchi-Hayashi K, Sekiguchi M, Ashigaki S, Takamatsu M, Hasegawa H, Suzuki-Migishima R, Yokoyama M, Nakanishi S, Tanabe Y. Generation of Reelin-Positive Marginal Zone Cells from the Caudomedial Wall of Telencephalic Vesicles. The Journal of Neuroscience, 2004; 24: 2286 –95
48 Meyer G, Perez-Garcia CG, Abraham H, Caput D. Expression of p73 and Reelin in the developing human cortex. J Neurosci 2002; 22: 4973-86
49 Radner S, Banos C, Bachay G, Li YN, Hunter DD, Brunken WJ, Yee KT. beta2 and gamma3 laminins are critical cortical basement membrane components: ablation of Lamb2 and Lamc3 genes disrupts cortical lamination and produces dysplasia. Developmental neurobiology 2013; 73: 209-29
50 Assadi AH, Zhang G, Beffert U, McNeil RS, Renfro AL, Niu S, Quattrocchi CC, Antalffy BA, Sheldon M, Armstrong DD, Wynshaw-Boris A, Herz J, D'Arcangelo G, Clark GD. Interaction of reelin signaling and Lis1 in brain development. Nature genetics 2003; 35: 270-6
51 Hirotsune S, Fleck MW, Gambello MJ, Bix GJ, Chen A, Clark GD, Ledbetter DH, McBain CJ, Wynshaw-Boris A. Graded reduction of Pafah1b1 (Lis1) activity results in neuronal migration defects and early embryonic lethality. Nature genetics 1998; 19: 333-9
52 Hong SE, Shugart YY, Huang DT, Shahwan SA, Grant PE, Hourihane JO, Martin ND, Walsh CA. Autosomal recessive lissencephaly with cerebellar hypoplasia is associated with human RELN mutations. Nat Genet 2000; 26: 93-6